Journal Pre-proof

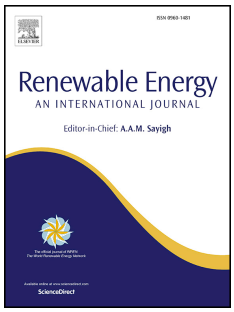

Experimental performance analysis of a novel sand coated and sand filled polycarbonate sheet based solar air collector

Biplab Das, Jayanta Deb Mondol, Sushant Negi, Mervyn Smyth, Adrian Pugsley

PII: S0960-1481(20)31620-7

DOI: https://doi.org/10.1016/j.renene.2020.10.054

Reference: RENE 14344

To appear in: *Renewable Energy*

Received Date: 15 July 2020

Revised Date: 5 October 2020

Accepted Date: 13 October 2020

Please cite this article as: Das B, Mondol JD, Negi S, Smyth M, Pugsley A, Experimental Performance Analysis of a Novel Sand Coated and Sand Filled Polycarbonate Sheet Based Solar Air Collector, *Renewable Energy*, https://doi.org/10.1016/j.renene.2020.10.054.

Experimental Performance Analysis of a Novel Sand Coated and Sand Filled Polycarbonate Sheet Based Solar Air Collector

Biplab Das[1,2*], Jayanta Deb Mondol[2], Sushant Negi[1], Mervyn Smyth[2], Adrian Pugsley[2]

[1]Department of Mechanical Engineering, NIT Slchar, Assam-788010, India

[2]Belfast School of Architecture and the Built Environment, CST, Ulster University, Northern Ireland, UK.

*Corresponding Email- b.das@ulster.ac.uk / biplab.2kmech@gmail.com

Sheet Based Solar Air Collector

Abstract:

An experiment was conducted to investigate the performance of a novel sand coated and sand filled (SCSF) polycarbonate sheet based solar air collector (SAC) under controlled indoor conditions with variable air flow rates and solar inputs. The performance of this novel absorber was compared with aluminium absorber (with and without sand coating). The results indicated that due to the presence of sand coating over the absorber, the rate of heat transfer was enhanced by redistribution of air flow. Further, the presence of sand within the poly carbonate sheet acted as a thermal heat storage medium that might be used during off-sunshine hours. Further, the increment in mass flow rate by 87% lead to decrement in the magnitudes of stored energy by 10-24% and but the average discharging efficiency was increased by 15%. The maximum thermal efficiency of the proposed collector was found to be 42% during charging. Reduction of air gap from 5 cm to 3 cm resulted in 11% higher thermal efficiency for sand coated aluminium absorber based SAC. It was found that the SAC with storage provided 39% and 20% higher thermal efficiency than that of the black paint coated aluminium absorber and sand coated aluminium absorber, respectively.

Keywords: *Solar air collector; sand coating; sensible heat storage; charging efficiency; discharging efficiency*

1. Introduction

Solar air collectors are widely used to transform the incoming solar radiation into useable form such as hot air, which can be used to dry agricultural products, space heating, and energy storage applications. The lower setup and operating cost of solar air collector (SAC) in comparison to other conventional energy sources make it more feasible solutions especially for the small-scale farmers. These types of collectors have many attractive advantages over water heating collectors such as higher working pressure range, fewer problems of corrosion or leakage, and non-freezing behaviour

of air, etc. [1, 2]. The worldwide distributions of solar thermal collectors based on type are as follows: vacuum tube heaters: 71.1%, flat plate collectors: 22.1%, unglazed water heaters: 6.3%, and solar air collectors 0.4% [3].

It is obvious that the thermal applications of SACs are still limited; due to poor heat transfer between the air and the absorber plate because of development of laminar sublayer and lower thermal capacity of air [4]. Moreover, cloudy weather conditions and off sunshine hours or night restricts the efficient use of SAC for agricultural drying and heating applications. The possible solution to overcome this issue is to provide heat storage capability so that thermal energy can be stored in the daytime, and later it can be used in night as well as in peak load hour. One of the effective ways to improve the heat transfer from absorber plates is surface modification, which helps to generate the secondary flow in the collector and increase the surface area. Das et al. [4] experimentally investigated the performance of SAC with sand coated absorber plate at variable air mass flow rate ranging from 0.01 to 0.02 kg/s/m^2 and radiation levels of 400, 600, and 800 W/m^2. Results indicated that the thermal efficiency of the collector improved by 17% for the sand coated absorber plate compared to the plain absorber, at a mass flow rate of 0.02 kg/s/m^2 and radiation level 800 W/m^2. Karwa and Srivastava [5] numerically investigated the effect of absorber plate with v-down discrete rib roughness on the thermal performance of SAC. The thermal efficiency of the SAC with roughened duct was obtained between 6% and 26% higher when compared to the performance of smooth duct SAC. Debnath et al. [6], Karim and Hawlader [7] found that use of corrugated absorber plate significantly improves the thermal performance of SAC, this was due to the improved turbulence effect and increment of the heat transfer area. Lati et al. [8] tested the performance of collectors with sand coated absorber plates. It was found that absorber plate coated with finer sand particles have better performance, maximum efficiency of 62.1 % was noticed when the sand particle diameter was 0.063 mm. Singh et al. [9] observed that SAC with circular jet impingement significantly enhances its thermal performance, and recommended to use bed porosity of 98%, mass flow rate of 0.04 kg/s, and impinging plate perforation of 0.48% to achieve best

performance of proposed SAC. Vaziri et al. [10] designed and tested SAC having different inner collector colors with and without glazing. The maximum efficiency of 85% at mass flow rate of 0.036kg/s was found for the black painted SAC with glazing. Velmurugan and Kalaivanan [11] studied the effect of four different geometrical arrangements such as wire mesh, finned plate, flat plate and rough plate on energy and exergy performance of SAC with single/dual pass. Wire mesh SAC with dual pass provided highest temperature of 25.2˚C and maximum efficiency of 76.46% than other conditions. Special selective coatings on the surface of absorber plate such as nickel-tin [12], mixture of vanadium and aluminium oxides [13] were also employed to obtain high effectiveness in solar air collectors.

Several researchers have also improved the performance of SACs by integrating it with heat storage media such as sensible or latent materials. The characteristics of latent heat storage such as high heat capacity and constant charging and discharging temperature make it more appealing; however poor thermal conductivity of these solid phase materials is one of the major drawbacks. Consequently, high thermal resistance has been noticed as the material deposits on the heat transfer surface during the discharging process [14]. Due to easier availability, lower cost, ease of fabrication, and higher thermal conductivity, the sensible storage materials are generally preferred over latent heat storage materials [15]. Kalaiarasi et al. [16] analysed the thermal performance of SAC with sensible heat storage medium such as synthetic oil (Therminol-55), and reported maximum thermal efficiency of 70.8%, when the mass flow rate was 0.028 kg/s. Saxena et al. [17] constructed SAC with heat storing media such as granular carbon and the maximum thermal efficiency of 73.6 % and 20.7 % was achieved under forced and natural convection mode, respectively. Laksmi et al. [18] experimentally investigated the performance of SAC with trapezoidal corrugated absorber plate and gravel as sensible heat storage media. The maximum energy efficiency was 58.16%, while the exergy efficiency was 14.6 %. Aissa et al. [19] used granite stones for developing a flat SAC with heat storage system, and measured the output of SAC by varying air mass flow rates from 0.016 kg/s to 0.08 kg/s under forced convection mode, They

concluded that the air mass flow rate in the range of 0.02-0.048 kg/s is the most suitable choice for achieving optimum outlet air temperature for the heating applications. Mohanraj and Chanderasekar [20] concluded that the sand with aluminium scraps as a packing material facilitates to maintain steady air temperature inside the drying chamber. Also, the inclusion of storage media has significantly increased the drying time by about 4 hours per day. Ramadan et al. [21] examined the thermal performance of SAC with limestone and gravel as heat storage materials, and observed that the gravel gave better results than lime stone. It is also observed that air mass flow rate up to 0.05 kg/s has shown increment in thermohydraulic efficiency, but beyond that it has insignificant effect, thus it is recommended to use mass flow rate equal to 0.05 kg /s or lower to have a lower pressure drop across the system. Murali et al. [22] outlined that use of aluminium cans with aluminium scraps as storage media for SAC gives better heat transfer coefficient and instantaneous efficiency, when the air mass flow rate was 0.025 kg/s. Abuska et al. [23] have measured the efficiency of SAC with cherry powder and cherry pits, and noticed that SAC with cherry pits have improved thermal efficiency of 27.03% in comparison to SAC with powdered cherry pits. Saxena et al. [24] experimentally investigated the use of SAC with granular carbon and mixed desert as sensible heat storage materials. Maximum thermal efficiency of 20.78 % and 80.05% was observed under natural and forced convection mode, respectively. Dhote and Thombre [25] determined the influence of change in inclination such as 0°, 15°, 30°, 45°, 60°, 75°, 90° and storage oil quantity such as 50, 75, 100 litre on the overall efficiency of SAC and the maximum efficiency was 16.88% at inclination of 60° and storage quantity of 50 litre. Chaouch et al. [26] developed a forced convection based solar dryer having pebbles as heat storage material. It was found that the efficiency of SAC with storage capability improved by 28% than the system without storage. The designed solar dryer was also very much capable of maintaining its efficiency for an hour after the sunset. Prasad et al. [27] performed their study using wire mesh as packing material to develop SAC, and further varied the air mass flow rate between 0.0159 and 0.0347 kg/s-m^2 to evaluate the heat transfer and friction characteristics. It has been observed that the heat transfer coefficient was increased with the

increase of mass flow rate and decrease in porosity. Abou-Ziyan et al. [28] highlighted that the thermal performance of the SAC with sensible storage materials was considerably higher than the system without storage. An optimum thickness of the storage material of about 0.12 m was found to be convenient for drying different agriculture products. The mathematical model of Naphon [29] showed that the thermal efficiency of SAC with porous media improved by 25.9 % than that of without porous media. Thakur et al. [30] enhanced the performance of SAC using wire mesh screens in layer by layer manner to fabricate the packed bed. It was observed that both friction factor and heat transfer coefficient were strongly influenced by the geometrical arrangements of wire mesh screens. Also, it was noticed that the volumetric heat transfer coefficient increased with the decrease in porosity. Saravanakumar and Mayilsamy [31] found that the thermal efficiency of SAC with gravel and iron was 20% higher in comparison to SAC with other types of selected storage materials. Moreover, the inclusion of heat storage materials increased the collector efficiency and outlet temperature by 10-20%. Vijayan et al. [32] developed a low cost solar air collector integrated with pebbles packed bed as sensible heat storage medium for the drying of bitter gourd slices. The average exergy efficiencies and pickup values were found in the range of 28.2-40.6% and 17.1-54.2% for the mass flow rates of 0.0141 kg/s to 0.0872 kg/s, respectively. A summary of performances of various solar air collectors using different sensible heat storage materials are presented in Table 1.

Although many researchers have discussed the performance enhancement of SAC by modifying the surface of absorber plate or employing sensible heat storage media, but research on the use of natural materials like as sand as coating and heat storage materials are scarce in literature. A few references [4, 8] show the performance of SACs using sand as coating material to modify the absorber's surface, while the references [20, 24, 28, 31] show the performance of SAC having sand as storage materials. But, none among those proposed designs have attempted to use sand as coating and heat storage materials (i.e., sand coated and sand filled) successively. Furthermore, multi walled polycarbonate sheet based SAC has not been well explored yet. Hence, this study

130 presents a novel sand coated and sand filed (SCSF) collector cum storage unit that includes
131 following key features: (i) black painted sand coating is used to modify the surface of the absorber
132 for better heat transfer; (ii) sand is used as sustainable and eco-compatible sensible heat storage
133 material; and (iii) multiwall poly carbonate sheet is used as base absorber material instead of
134 traditional aluminium/copper absorber plate. Finally, the performance of proposed SAC was
135 compared with the traditional black painted sand coated aluminium absorber under similar working
136 conditions.

137 2. Experimental set up

138 In the present study sand is considered as the thermal storage materials for evaluating the thermal
139 performance of the sustainable and eco-compatible solar air collector. The primary aim was to
140 heating air using solar energy and to incorporate storage system so that thermal energy can be
141 stored in the daytime, and later it can be used in night as well as in peak load hour to maintain the
142 air temperature. The main experimental setup consists of black painted sand coated polycarbonate
143 sheet filled with sand (Fig. 1a). Further, the previously made thermal collector presented by Das et
144 al. [4] is used with modified air gap for comparison. The function of the polycarbonate sheet was
145 twofold: the upper surface acts as an absorber while the multiwall helps to store the sand thus the
146 combined system acts as a collector cum storage. Further, the presence of sand controls to maintain
147 the temperature of the polycarbonate reaching at higher level thus reduces the chances of
148 degradability under higher solar insolation. Differential Scanning Calorimetry (DSC) was used to
149 derive information regarding the amount of heat required to increase the sample temperature. The
150 heat flow (mW) function with a blank curve correction was provided for samples heated at 5^{o}C per
151 minute under N_2 environment from 30 to 600^{o}C as displayed in Fig. 1b. The DSC analysis of pure
152 sand is performed to study the crystallization process and latent heat involved in the process. A
153 sharp downfall in the heat flow is recorded with a peak position located at $\sim 575\ ^{0}$C which
154 demonstrates the crystallization of the materials due to the exothermic process. This phenomena is

155 explained based on the flow of heat energy to the sample which is reduced to keep the heating rate

156 constant.

157

158

159

160 **Fig. 1. Pictorial view of the experimental setup. (a) Frame of the collector; (b) Sand filled polycarbonate sheet;**
161 **(c) Side view of the collector under the solar simulator; (d) Solar simulator and collector during**
162 **experimentation; (e) Temperature sensors, data logger, voltage variac, computer for online storing; (f) Voltage**
163 **regulator for simulator.**

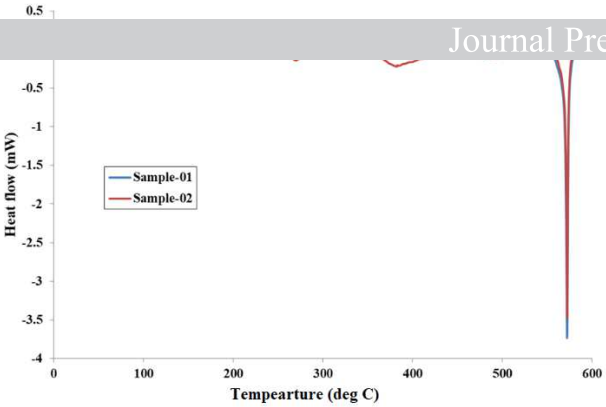

Fig. 1g. DSC analysis of sand.

The experimental setup of the SCSF collar collector can be seen in Fig. 1. The collector has a cross-sectional area of 1.44 m^2 and an absorber plate of 0.97 m x 0.97 m. Further, all the technical specifications of the storage based solar collector kept same as that of Das et al. [4]. However, to adjust the thickness of the multi-wall polycarbonate sheet having thickness of 0.02 m, the air gap was reduced to 0.03 m compared to that of the 0.05 m for the case of Das et al. [4]. The back side was insulated by using 0.02 m thick Thermocol. The outer body of the collector was made of 0.015 m thick plywood. The top surface of the polycarbonate sheet was first coated with black paint and then a layer of black painted sand was coated over it. To make the sand coating, mixture of black paint and preheated sand were painted over the absorber. For the storage, the dried sand was inserted in between the multi-walls of the polycarbonate sheet. A single transparent glazing made up of Perspex sheet having thickness of 0.005 m was employed to reduce the top losses. Two DC fans each of 12V capacity were utilised to blow the air from the bottom (considered as the inlet) of the collector. A voltage variac was used to supply controlled DC power to the fans.

Solar simulator with variable radiation level of 800 W/m^2 and 400 W/m^2 are used as a source of light and tests are performed at the laboratory of Centre for Sustainable Technologies, Ulster University. The radiation level was measured by a pyranometer by keeping it at different position of the collector. The average intensity on the collector surface varied between ±15 W/m^2. The collector and simulator lamp array were kept parallel to each other and were at 45º inclined to horizontal. The exit air velocity was measured with the help of an anemometer and the velocity was

varied by varying the speed for the fan. Data logger (data taker, DT85) was used to read and store the temperature reading at an interval of 1 minute. The accuracy of the instruments and the involved uncertainties were evaluated using equations reported by Das et al. [4] and the values are shown in Table 2.

Table 2: Accuracy and percentage errors for various instruments.

Instrument	Make/ Model	Accuracy	Range	% error
Pyranometer	Kipp & Zonen	± 5 W/m^2	0 – 4000 W/m^2	2.5
Anemometer	Trotec, TA300	± 0.01 m/s	0 – 25 m/s	0.5
Differential manometer	OMEGA, HHC280	± 0.05 hpa	0-100 hpa	5
T-type thermocouple	Laboratory of Ulster university	± 0.5^{0}C	0 – 300 ^{0}C	1.25

3. Mathematical formulation

Steady flow energy equation for solar air collectors is given by [4, 8]

Accumulated energy (Q_{ac}) = Useful heat energy gain (Q_u) + Absorbed energy by the absorber/storage (Q_{ab}) + Lost energy (Q_{loss}) (1)

Accumulated energy can be evaluated as:

$$Q_{ac} = I A_c \quad (2)$$

where, I is the magnitudes of the solar radiation and A_c is the collector area.

Useful heat gain by the moving air is evaluated as:

203 $Q_u = m_a C_{p,a}(T_{a,out} - T_{a,in})$ (3)

204 where, m_a is the air mass flow rate, $C_{p,a}$ is the specific heat of air, $T_{a,out}$ is the outlet air temperature
205 and $T_{a,in}$ is the inlet air temperature.

206 The absorbed energy in the storage (Q_{ab}) is calculated by

207 $$Q_{ab}=m_p C_{p,s}(dT_{p,average}/dt) \quad (4)$$

208 where, m_p is the mass of the sensible storage material (i.e., sand), $C_{p,s}$ is the specific heat of sand,
209 $dT_{p,average}$ is the change in average temperature of the sand during time gap of dt.

210 The energy loss (Q_{loss}) is given by

211 $$Q_{loss}= U_c A_{sc}(T_{p,average}-T_e) \quad (5)$$

212 where, U_c is the overall heat loss coefficient, A_{sc} is the area of the absorber, $T_{p,average}$ is the average
213 temperature of sand air, and T_e is the temperature of the environment.

214 The air mass flow rate can be evaluated as

215 $$m=\rho A_{sc} V \quad (6)$$

216 where, ρ is the density of the air and V is the air speed.

217 The thermal performance of the SCSF polycarbonate sheet based SAC is based on the heat transfer
218 from the hot air to the sand in the reservoir and vis versa. The charging efficiency or storing
219 efficiency ($\eta_{s,c}$) is estimated from the ratio of the amount of stored energy in the sand to the total
220 amount of incident solar radiation.

221 $$\eta_{s,c}= Q_{ab}/ IA_{sc} \quad (7)$$

222 In storage based solar collector systems, two different thermal efficiencies can be calculated: heat
223 collection (charge) efficiency and heat retrieval (discharge) efficiency.

224 The thermal efficiency of the collectors ($\eta_{t,c}$) during charging is defined as the ratio of the total
225 quantity of heat transferred to the air and the total solar irradiance incident [28].

The thermal efficiency of the collectors ($\eta_{t,d}$) during discharging is defined as the ratio of the total quantity of heat transferred to the air and the total energy stored in the storage (Q_{ab}).

$$\eta_{t,d}=Q_u/(Q_{ab}) \quad (9)$$

4. Results and discussion

4.1. Charging mode

4.1.1. Variation of temperature difference

The variation in temperature difference between the glazing and the inlet air (*ΔT_glazing*), the absorber and the inlet air (*ΔT_absorber*), and the outlet air and the inlet air (*ΔT_air*) with time is shown in Fig. 2a-d. At a lower mass flow rate of 0.0096 kg/s and at lower radiation level of 400 W/m^2, a continuous increase in the magnitude of the temperature differences is observed with time. Results also indicated that *ΔT_absorber* is always higher than the other values (*ΔT_air* and *ΔT_glazing*). This may be due to the lower rate of heat transfer by the air. Conversely, lower values of *ΔT_glazing* is an indication of lower values of top heat loss from the collector. With the increase in mass flow rate to 0.018 kg/s (Fig. 2b), the magnitude of all temperature differences are found to reduce, due to an increase in the heat extraction rate by the working fluid (air). Furthermore, it is observed that the magnitude of *ΔT_air* and *ΔT_glazing* are similar. This may be due to higher rate of reduction of the outlet air temperature compared to that of the glazing temperature. Again, a reduction in the outlet air temperature is due to the lower retention time of the air within the collector due to the increase in the mass flow rate. At higher level of radiation (800 W/m^2), the trend remains the same but the values increase. The values of *ΔT_absorber*, *ΔT_air*, and *ΔT_glazing* are found to be in the ranges of between 16 to 35ºC, 8 to 25ºC, and 9 to 17ºC,

respectively. An increase in the mass flow rate of air by 87% results in a reduction in the outlet air temperature by 38% and 64% at lower and higher levels of solar radiation, respectively.

4.1.2. Variation of storage temperature and stored energy

The variation of the average storage (sand) temperature at three different positions with respect to time are shown in Fig. 3a-d for two different solar radiation levels. Positions are fixed along the axial direction near the inlet (referred to as T_{bottom}), midsection (referred to as T_{middle}) and near the exit (referred to as T_{top}). Each temperature reading is the average of three different sensors fitted in the radial direction at the same axial location. Results indicated that the temperature of the sand initially increases rapidly in the initial 50 min. due to the absorbance of solar radiation. Thereafter the rate of increase reduces due to an increase in the temperature difference between the incoming air and the temperature of the absorber resulting in a higher rate of extraction of heat by the travelling air. It is noted that the differences in temperature between the three locations increases with time. The maximum average storage temperature of 54ºC is observed with a maximum deviation of 4ºC between the inlet and outlet sections. Furthermore, with the increase in the mass flow rate to 0.018 kg/s (Fig. 3b), the maximum average temperature is 47ºC with a maximum deviation of 2ºC. Apart from the magnitude, a similar trend is observed at the higher radiation level of 800W/m^2 (see Fig. 3c-d). As can be seen, the maximum temperature varies between 70 to 84ºC. However, the deviation in temperature between the inlet and outlet varies between 6 and 8 ºC. This deviation is due to the reduction in the driving force (i.e. temperature difference between the air and the absorber) and thus the heat absorption capacity of the fluid as it moves in the axial direction. Eventually the axial temperature of air increases gradually.

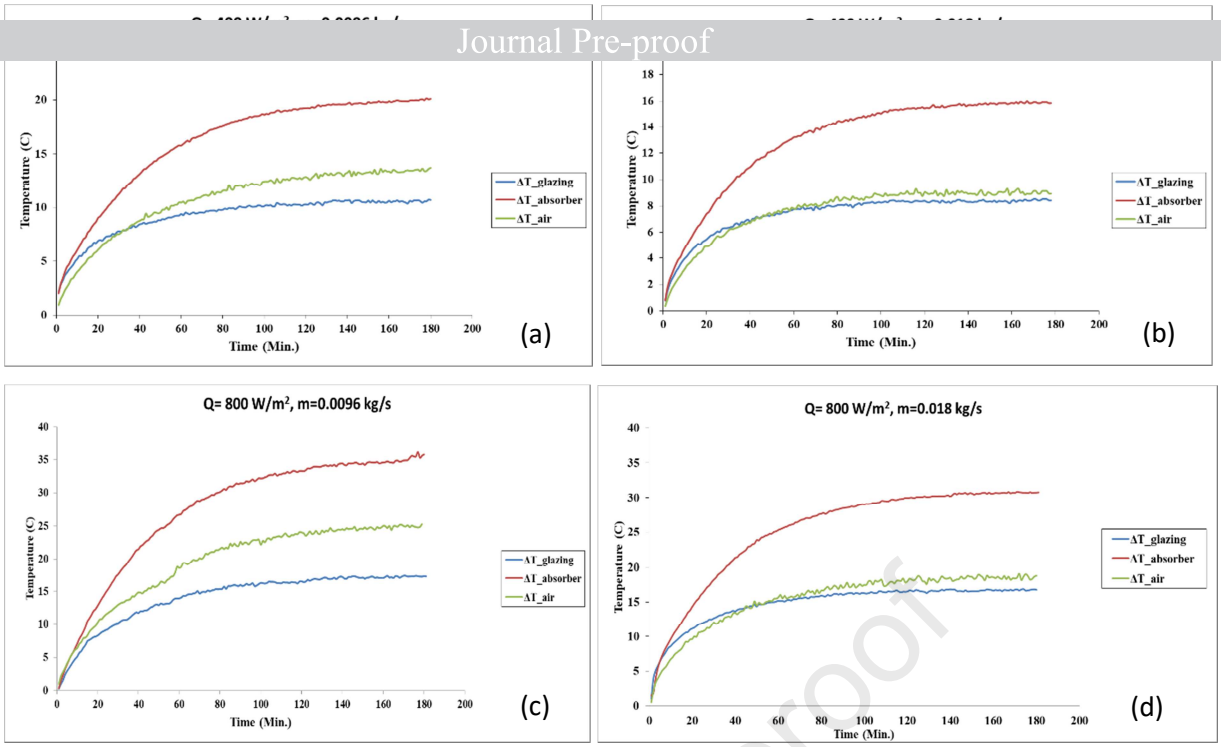

Fig. 2. Variation of temperature difference. (a) Q=400 W/m^2, m=0.0096 kg/s; (b) Q=400 W/m^2, m=0.018 kg/s; (c) Q=800 W/m^2, m=0.0096 kg/s; (d) Q=800 W/m^2, m=0.018 kg/s.

Variation of the total stored energy in the sand with time is shown in Fig. 4a-b. As can be seen, the magnitude of stored energy increases with time due to absorption of solar radiation. Initially, the rate of increase is high due to higher absorption capacity of the sand because of the lower temperature. With the passage of time, the surface temperature of the absorber (and thus the storage temperature) increases resulting in a higher rate of extraction of heat by the air. At the same time due to higher system temperature, the level of the top (leakage) losses increases. At lower levels of solar radiation (400 W/m^2), the increase in the air mass flow rate results in a decrease in the levels of the heat storage rate due to the higher rate of heat extraction by the flowing air. This may be due to lower potential retention of the flowing air that allows the sand to store more energy. At higher solar radiation levels (800 W/m^2), the variation with time is similar to lower solar radiation, but the amount of stored energy is higher. Furthermore, the increase in air mass flow rate resulted in a decrease in the stored energy for all mass flow rates, mainly due to the increase in extraction rate of thermal energy. Overall, the stored energy decreased by 10 to 24% for an increase in air mass flow rate by 87%.

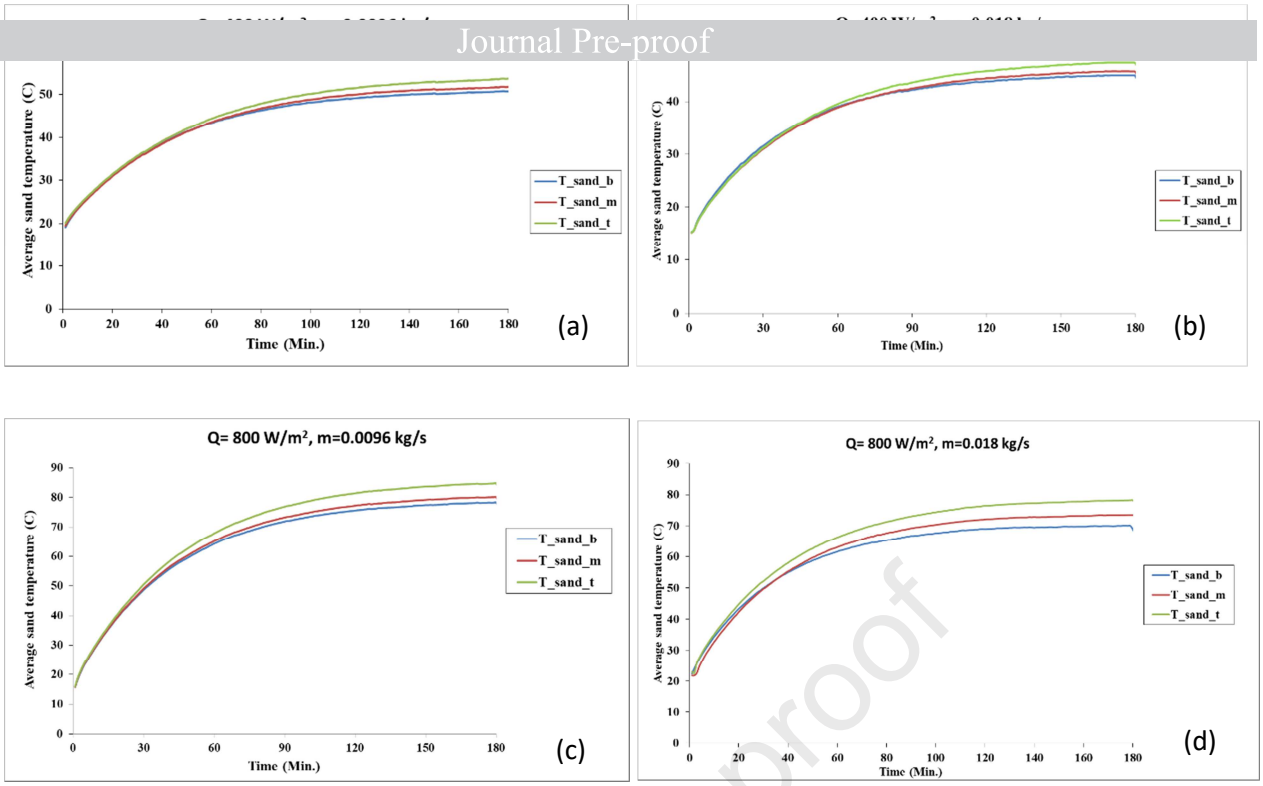

Fig. 3. Variation of average storage (sand) temperature during charging. (a) Q=400 W/m^2, m=0.0096 kg/s; (b) Q=400 W/m^2, m=0.018 kg/s; (c) Q=800 W/m^2, m=0.0096 kg/s; (d) Q=800 W/m^2, m=0.018 kg/s.

4.1.3. Variation of charging efficiency

The variation in charging efficiency with time for various mass flow rates of air is depicted in Fig. 5a-b. As can be seen, the charging efficiency initially increases but this is followed by a drop off over time. It may be inferred that from the total incident radiation, a portion of the heat is stored in the sand, a portion is absorbed by the flowing air and remainder is lost. An initial increase in the charging efficiency resulted from the increase in the magnitude of heat stored in the sand. And a comparatively lower amount of heat carried away by the travelling air due to lower temperature gradient between the incoming air and the surface of the absorber. Further, with the passage of time, the increase in heat storage within the sand increases the surface temperature of the absorber which in turn increases the amount of heat extracted by the flowing air.

It is important to mention here that higher system temperature also results in higher heat loss to the environment. Since the primary aim of the present setup is to use it as a collector, thus the lower value of charging efficiency can be accepted, if the conversion efficiency of the collector

is enhanced with the variation of any of the governing parameters. Results indicate that after almost 60 min., the fraction of heat absorbed by the flowing air and the sand takes a steady trend. The initial increase in air mass flow rate, leads to increase in heat absorbing capacity of the travelling air, resulting in a lower value of maximum charging efficiency. Thus, it can be concluded that a mass flow rate of 0.0012 kg/s is better in terms of charging efficiency of the collector. The variation of the charging efficiency at a higher intensity (800 W/m^2) shows similar trend to the low intensity (400 W/m^2) (Fig. 5b). The deviation of the charging efficiency becomes insignificant after a certain time for all the air mass flow rate.

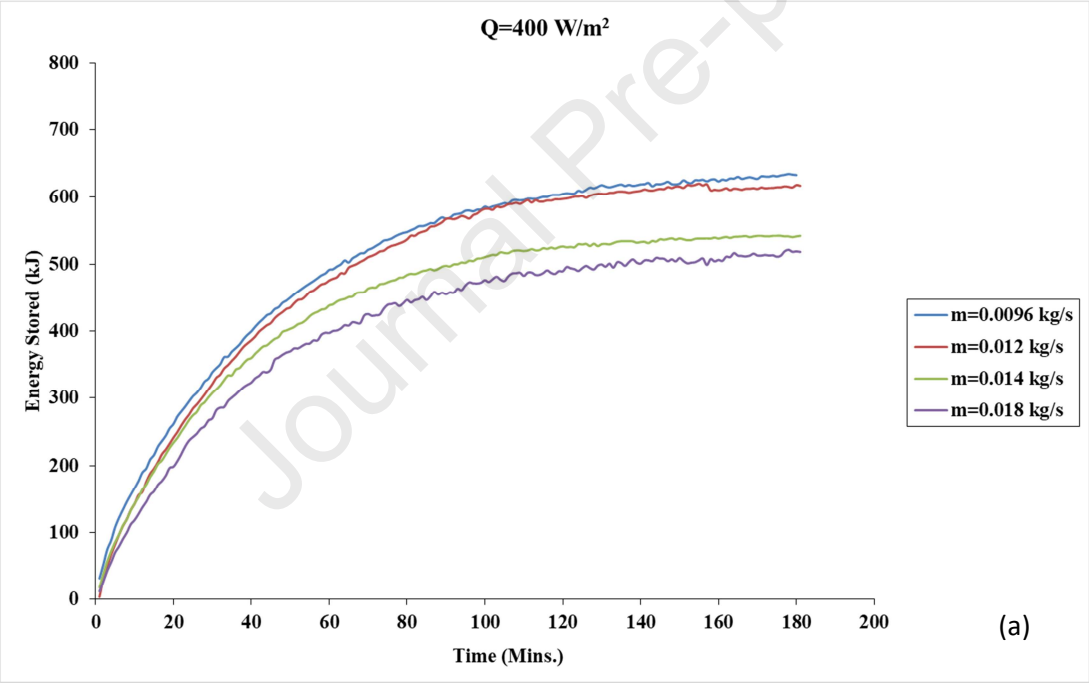

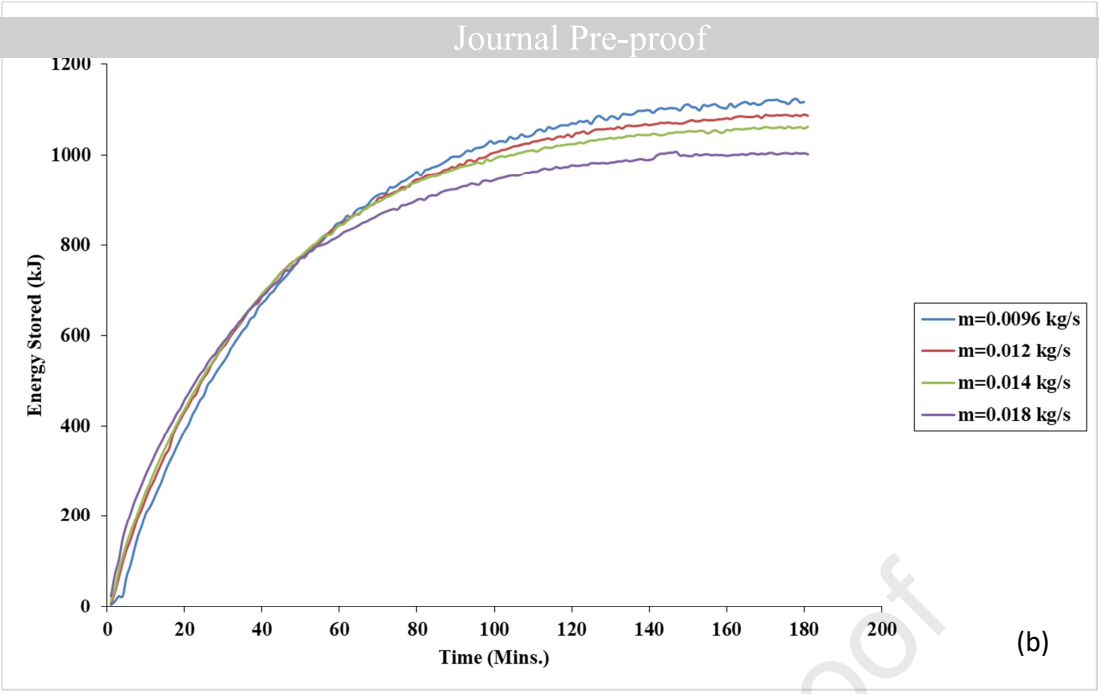

Fig. 4. Variation of average stored energy at different mass flow arte of air. (a) Q=400 W/m^2; (b) Q=800 W/m^2.

4.1.4. Variation of thermal efficiency during charging

The variation of thermal efficiency of the collectors with time at various air mass flow rates is shown in Fig. 6a-b. In general, the collector efficiency is found to increase with time and the rate of increase is higher at the beginning and thereafter it tends to reduce. With time, the surface temperature of the absorber increases due to absorption of incident solar radiation resulting in an increase in the temperature difference between the inlet air and absorber. But after some time, the heat extraction capacity of the flowing air reaches saturation and thus a reduction in the rate of increase is observed. Moreover, the amount of heat lost also plays a decisive role at higher absorber/system temperatures [2] as the amount of the top (leakage) heat losses is directly proportional to the system temperature. Results indicate that the increase in air mass flow rate helps to enhance the thermal efficiency due to better mixing of air within the collector. The maximum thermal efficiency was found to be 40% and 42% for 400 and 800 W/m^2, respectively, at air mass flow rates of 0.018 kg/s. It can be seen from Fig. 6a-b, that the increase in air mass flow rate by

335 97% enhanced the thermal efficiency by 52% and 50% at lower and higher solar radiation levels,

336 respectively.

337 It may be said from the energy balance it is clear that the total energy accumulated on the
338 solar collector is being used to enhance the temperature of the absorber and other components of
339 the collector. Further, since the absorber is attached with the sand (acting as a storage), thus,
340 increase in temperature of the absorber is linked with the increase in the temperature of the storage.
341 The travelling air gets heat up by taking heat from the absorber. In the beginning, on one side the
342 inlet insolation is mostly used to increase the temperature of the absorber and thus the storage. On
343 the other side, until the temperature of the absorber is increased to a certain value, due to lower
344 temperature gradient between the inlet air and the absorber, travelling air is unable to extract much
345 heat. These combined factors are the reasons for initial peak in the value of charging efficiency,
346 which is a ratio of heat absorbed by the storage to the total energy accumulated in the collector.
347 However, with passage of time, as the temperature of the absorber cum storage is increased, the
348 amount of energy carried away by the travelling air gets increased. This finally results in increase of
349 the thermal efficiency of the SAC and during this period of time, the charging efficiency remains
350 lower.

351

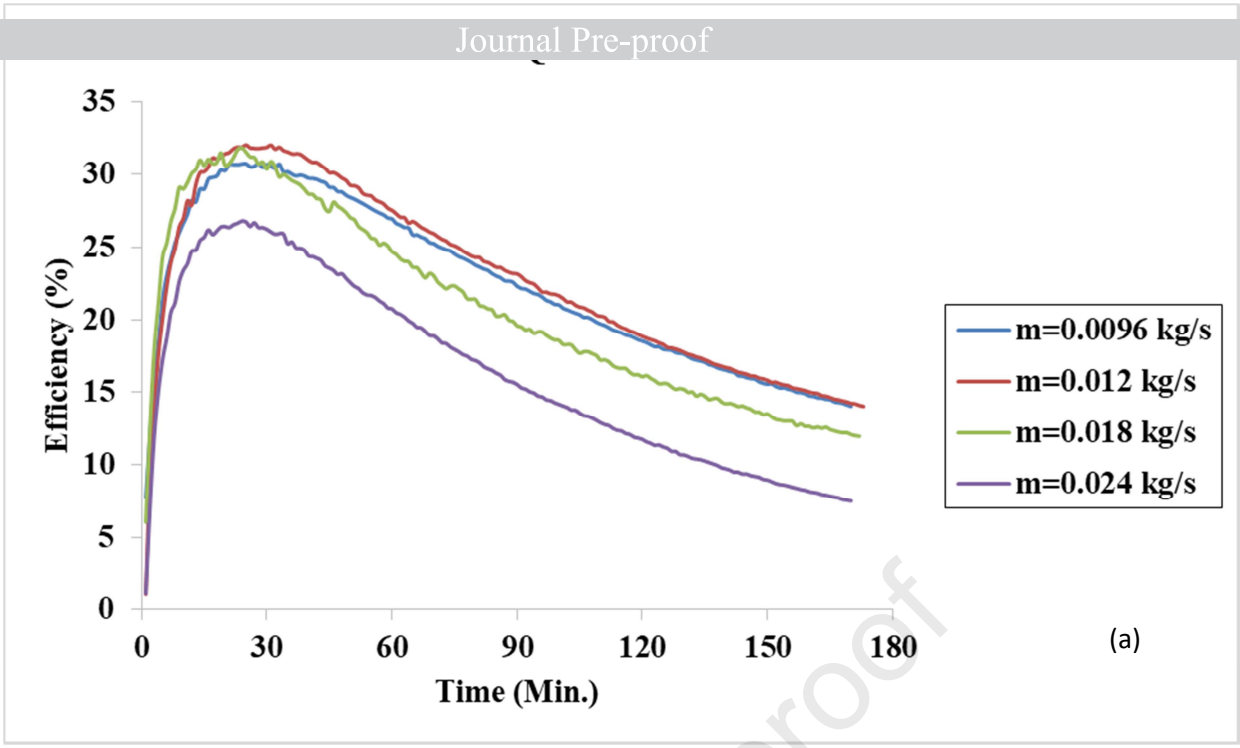

352

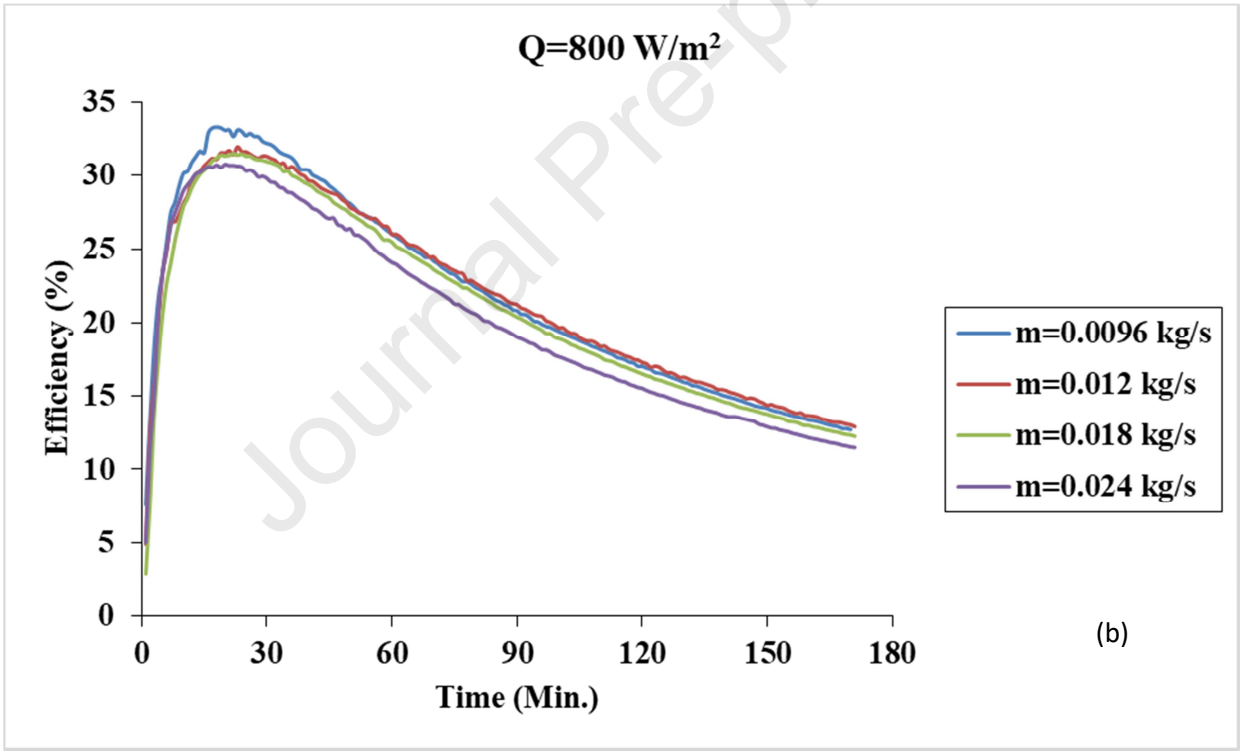

353

354 **Fig. 5. Variation of charging efficiency. (a) Q=400 W/m^2; (b) Q=800 W/m^2.**

355

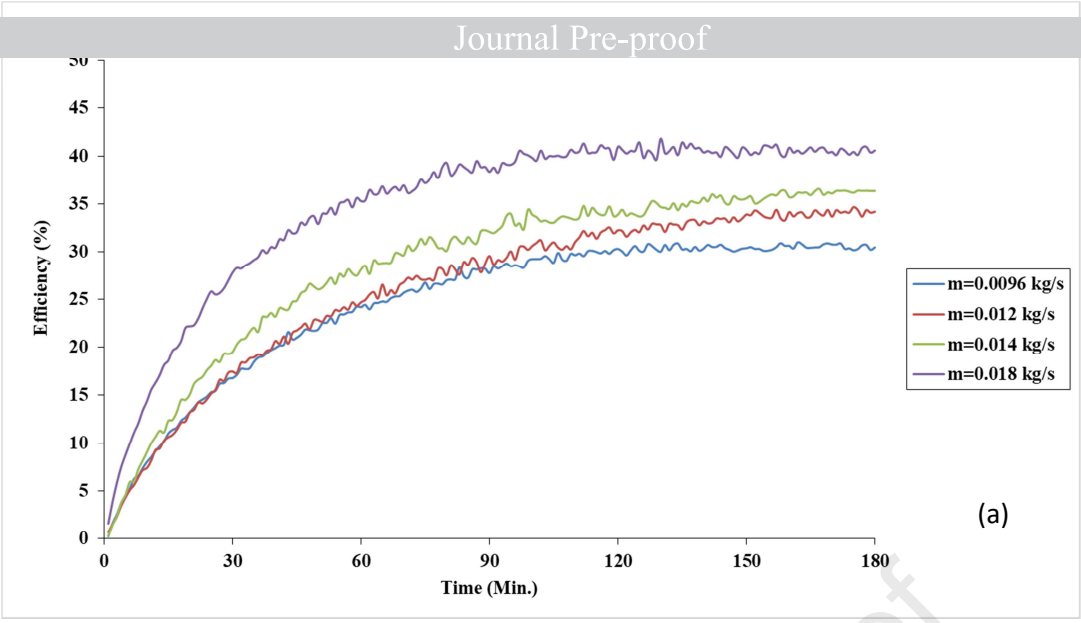

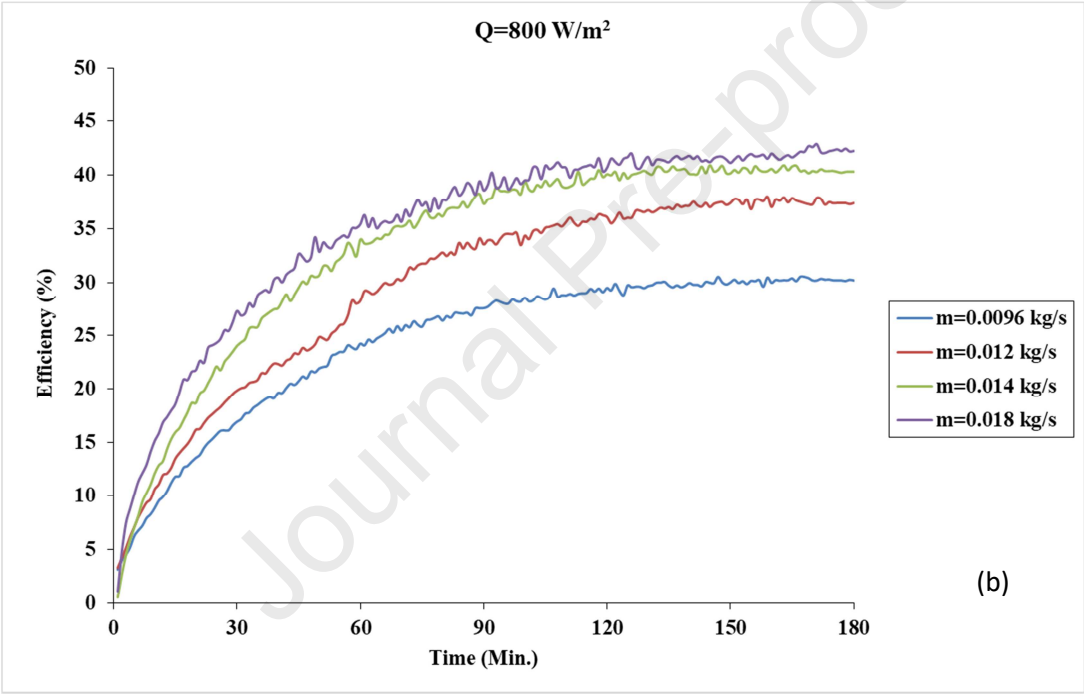

Fig. 6. Variation of thermal efficiency during charging. (a) Q=400 W/m^2; (b) Q=800 W/m^2.

4.2. Discharging Mode

4.2.1. Average sand temperature

The variation of average storage (sand) temperature during the discharging mode at different axial positions is shown in Fig. 7a-d. The positions are identical to that in the charging mode (Fig. 3a-d). As can be seen that the trend of decrease in temperature is similar during discharging to that of the

charging mode. The outlet temperature remains higher than the inlet due to the increase in temperature of the flowing air and that results in a reduction of heat absorbing capacity of the fluid in the downstream. An increase in the air mass flow rate results in lower storage temperature during charging but during discharging it extracts heat at a faster rate. The total charging time was around 180 min., whereas, the discharging time was around 120 min. Results indicate that for the collector charged at lower intensity (400 W/m^2) the sand temperature approaches to the surrounding environmental temperature (25 ºC) after 50 to 60 min. of discharging. The discharge rate is faster at a higher mass flow rate. At higher intensity, the trend is very similar to that of the lower intensity conditions, except that the sand temperatures attains higher values. Results showed that it took around 120 min. for the sand temperature to drop to ambient levels at a low air mass flow rate and around 100 to 110 min. at higher mass flow rate.

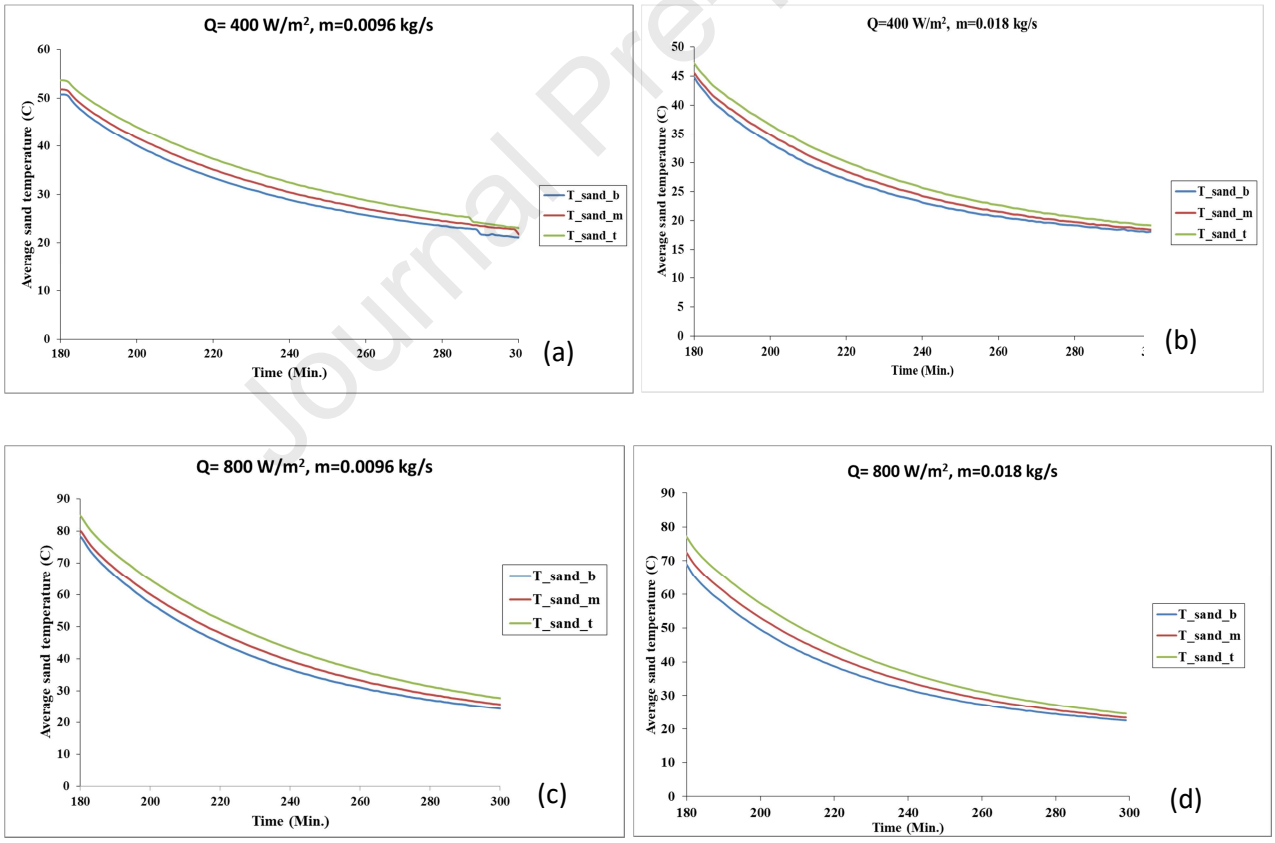

Fig. 7. Variation of average storage (sand) temperature during discharging. (a) *Q*=400 W/m^2, *m*=0.0096 kg/s; (b) *Q*=400 W/m^2, *m*=0.018 kg/s; (c) *Q*=800 W/m^2, *m*=0.0096 kg/s; (d) *Q*=800 W/m^2, *m*=0.018 kg/s.

4.2.2. Discharging of the stored energy

The variation in the percentage of energy discharged for different intensities is depicted in Fig. 8a-b. The total amount of stored energy during charging at a lower intensity of radiation is always lower than that at a higher intensity due to the amount energy incident on the absorber. Furthermore, at a lower mass flow rate the amount of energy stored is higher, due to lower rate of heat extraction by the flowing air (see Fig. 8a-b). During discharge, the rate of extraction of heat from the stored energy (sand) is always higher at higher mass flow rates. Furthermore, a quantitative comparison of lower and higher intensities indicates that the rate of percentage discharge is comparatively higher for the system when charged at a lower level of radiation. For an example, for a mass flow rate of 0.018 kg/s, almost 50% of the stored energy is discharged after 32 min. at lower intensity of radiation, whereas it takes almost 40 min., while charging at a higher intensity. The thermal energy stored in the sand is negligible after 80 min. of discharged period at lower intensity test conditions.

4.2.3. Average discharging efficiency

The variation of the average discharging efficiency is shown in Fig. 9. The discharging efficiency is the representation of the conversion of stored energy into useful heat. Results indicate that the increase in the air mass flow rate from 0.0096 kg/s to 0.012 kg/s resulted in an increase in the discharging efficiency due to better and faster extraction of the heat. This may also be linked with two factors: one is the magnitude of stored energy reduces with the increase mass flow rate of air; and other is the reduction in the temperature of the storage which helps to reduce the top losses. A further increase in the mass flow rate up to 0.018 kg/s resulted in monotonic decrease of the discharging efficiency by up to 9% compared to that at 0.0096 kg/s. This is due to the faster rate of discharge of stored energy at higher air mass flow rates.

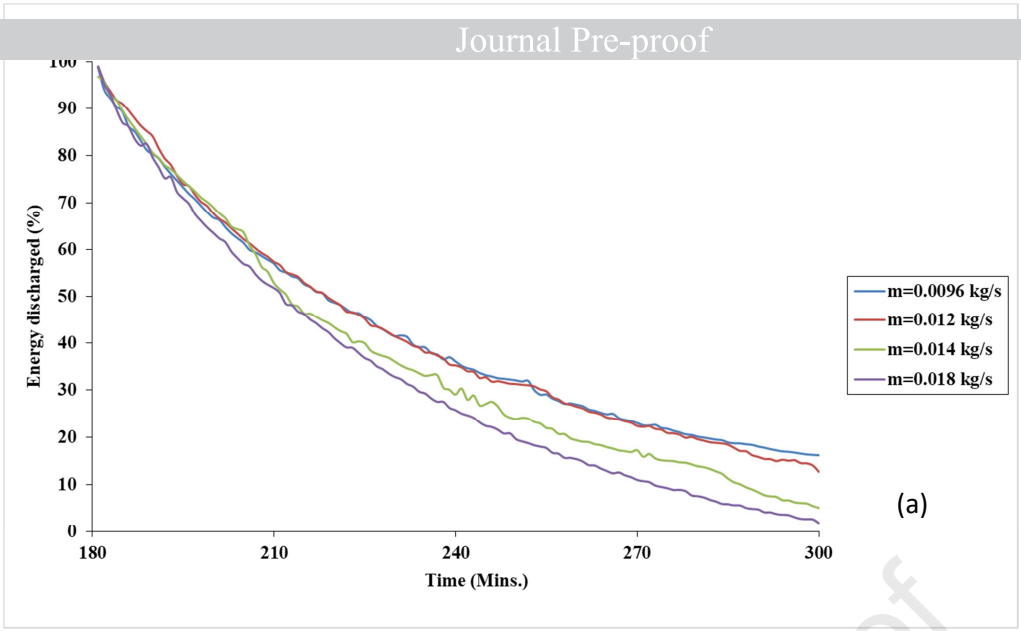

406

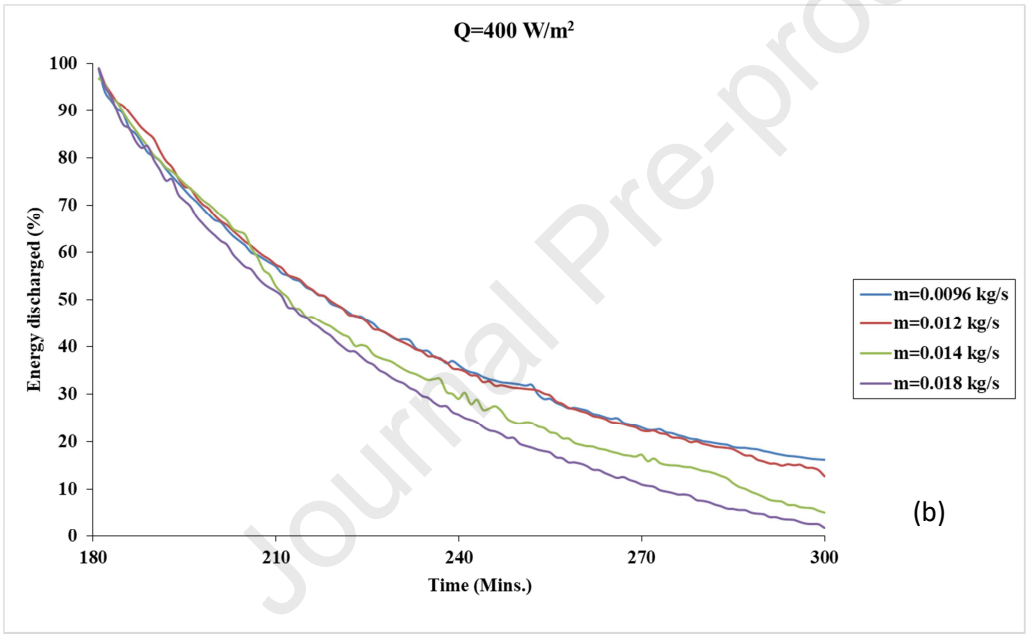

407

408 **Fig. 8. Percentage variation of energy discharged. (a) Q=400 W/m^2; (b) Q=800 W/m^2.**

409 At higher levels of radiation intensity, increasing the mass flow rate from 0.0096 to 0.012
410 kg/s results in increase in the discharging efficiency by almost 15%. It is important to mention that
411 at higher levels of radiation, the amount of losses are also high due to a higher system temperature.
412 Thus, an increase in the mass flow rate of air extracts more heat and reduces the system temperature
413 resulting in decrease in top (leakage) losses. These combined factors might be the reasons for a
414 higher rate of increase in discharging efficiency at higher radiation intensities. However, a further
415 increase in the air mass flow rate up to 0.018 kg/s resulted in a continuous decrease in the

discharging efficiency by up to 2% compared to that at 0.0096 kg/s. This indicates that the discharging efficiency depends on the air mass flow rate, and it reaches a maximum at a certain flow rate. In addition, an increase in the air mass flow rate not only decreases the discharging efficiency but also reduces the desired output temperature of the flowing air.

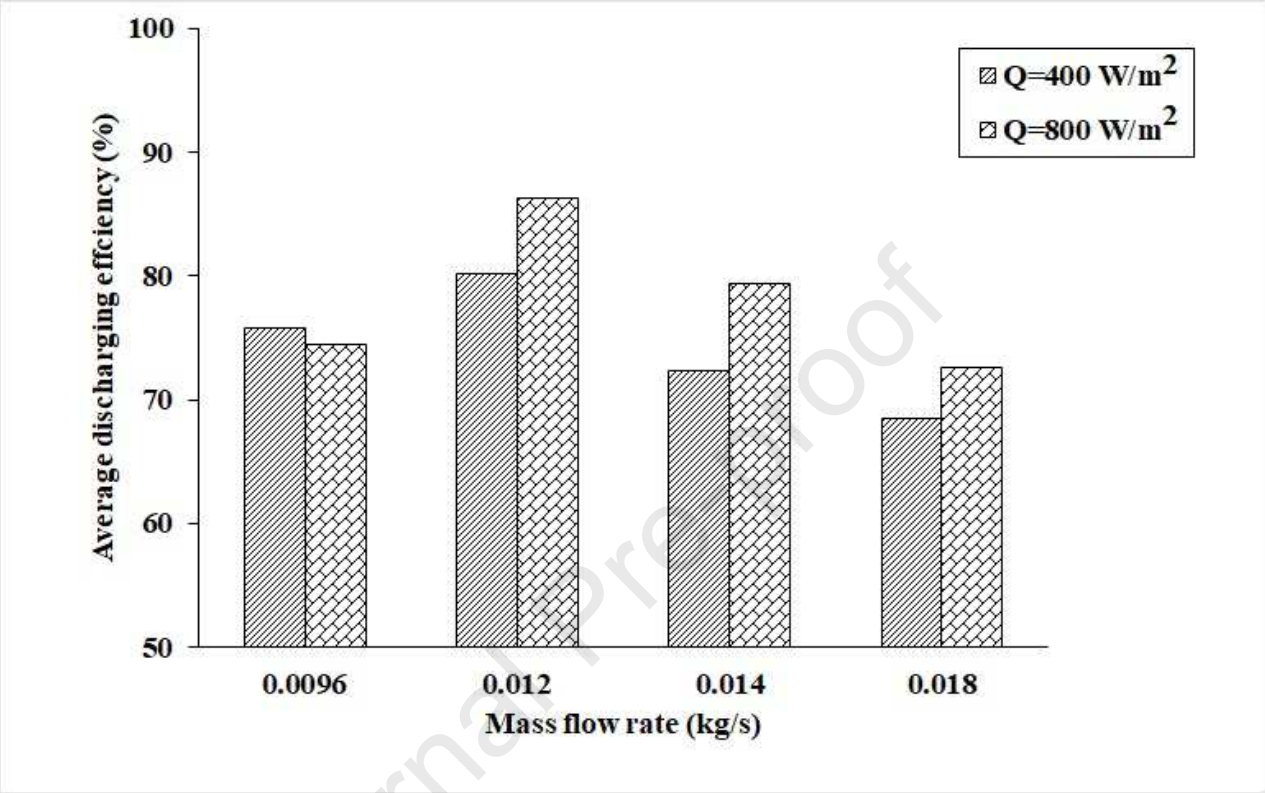

Fig. 9. Variation of average discharging efficiency.

4.3. Comparative variation of output temperature and thermal efficiency

The variation of thermal efficiency (η) and the corresponding output temperature (T) with air mass flow rate is presented in Figs. 10a-b. The data having notation 'black' and '*sand_5cm*' hass taken from Das et al. [4], representing the collector with an aluminium absorber coated with only black paint and sand coated with an air gap of 5 cm. The air gap for the present study was reduced to 3 cm due to the use of the polycarbonate sheet (noted as '*poly*'). Furthermore, for comparison

purposes, the same experiments were repeated with a sand coated absorber with an air gap of 3 cm, noted as '*sand_3cm*'.

At lower solar insolation levels (Fig. 10a), the results reveal that in general the efficiency increases with the increase in the air mass flow rate due to the better heat extraction. This is a result of better mixing of the fluid coupled with an increase in the heat extraction capacity of the flowing air. Furthermore, the presence of the sand coating in the absorber improves the heat transfer and the corresponding collector efficiency by almost 28% over that of the black coated absorber (with a 3 cm air gap) at lower air mass flow rates. The increase in efficiency with the sand coating is up to 13%, at higher air mass flow rate. Absorption of solar radiation by the successive layers of sand on the absorber surface acting as a volumetric phenomenon as compared to the surface phenomenon in case of the conventional collector [8]. Furthermore, the presence of the sand coating helps to increase the level of turbulence [4] which results in better mixing of the fluid which in turn increases the thermal efficiency by up to 17% [4]. The trend in the output temperature is in line with the trend of efficiency. With the increase in the air mass flow rate, the output temperature drops continuously due to the lower retention time of the flowing air. However part of the reduction of the total heat transfer due to reduction of output temperature is partially overcome by the increase in the air mass flow rate.

The reduction in the air gap from 5 cm to 3 cm provided an 11% higher efficiency at lower air mass flow rates (Fig. 10a). With higher air gaps, the total amount of fluid retained in the collector is higher and most of the flowing fluid tends to pass through the less resistive zone in between the absorber and glazing. Furthermore, at lower air mass flow rates, the air temperature is comparatively higher in the convection mode of heat transfer which plays an important role within the air gap. This results in higher convection losses through the glazing due to cross stream flow within the air gap, especially at wider air gaps. At higher air mass flow rates, due to lower temperature of the system, the level of convection losses tends to reduce due to the restricted cross-stream flow, which also indicates the dominance of forced convection, especially at higher air gaps.

A combination of these factors might be the reason for the improvement in the thermal efficiency of the collector by around 5% at higher air gaps and higher air mass flow rates of 0.014 kg/s.

Regarding the sand coated sand filled (SCSF) polycarbonate sheet based absorber, at lower levels of insolation (Fig. 10a), a continuous improvement in the performance of the collector is observed as compared to the traditional flat plate collector. The reduction of back losses in the presence of storage based absorber, and also the reduction of top losses due to lower surface temperature of the absorber might be the reason for the same. As can be seen, with a mass flow rate of 0.0096 kg/s and radiation level of 400 W/m^2, the value of $\Delta T_{\_absorber}$ is around 20ºC with the polycarbonate based absorber (Fig. 2a), whereas, the same temperature position is around 35ºC for the sand coated aluminium based absorber [4]. Overall the sand coated sand filled polycarbonate sheet based absorber provided up to a 39% improvement in efficiency at a lower mass flow rate of 0.0096 kg/s than that of the black paint coated aluminium absorber and 20% higher than the sand coated aluminium absorber. For an air velocity of around 0.9 m/s with Granular carbon added solar air collector the maximum temperature of 37.4 ºC was observed by Saxena et al. [7].

At a higher intensity (800 W/m^2), the trend of efficiency and output temperatures are almost the same (Fig. 10b), except the magnitude. Results showed that at a lower mass flow rate of 0.0096 kg/s, the thermal efficiency of the sand coated sand filled (SCSF) polycarbonate sheet based absorber is almost 40.5% and 25% higher than that of the black paint coated aluminium absorber and sand coated aluminium absorber, respectively. However, at a higher mass flow rate of 0.018 kg/s, the sand coated absorber with an air gap of 5 cm provided the highest efficiency. This is due to the dominance of forced convection coupled with comparatively lower absorber surface temperature since part of the heat is being absorbed by the sand storage. Furthermore, compared to lower levels of radiation, the collector efficiency for 5 cm air gap is lower than that for the 3 cm air gap at a mass flow rate of 0.014 kg/s. This is an indication of dominance of natural convection at higher levels of solar radiation. Lakshmi et al. [18] had reported that for solar air collector having

481 trapezoidal absorber and sand storage provided up to 26% of thermal efficiency under the outdoor

482 conditions, as that of the highest efficiency of 42% in the present case.

483

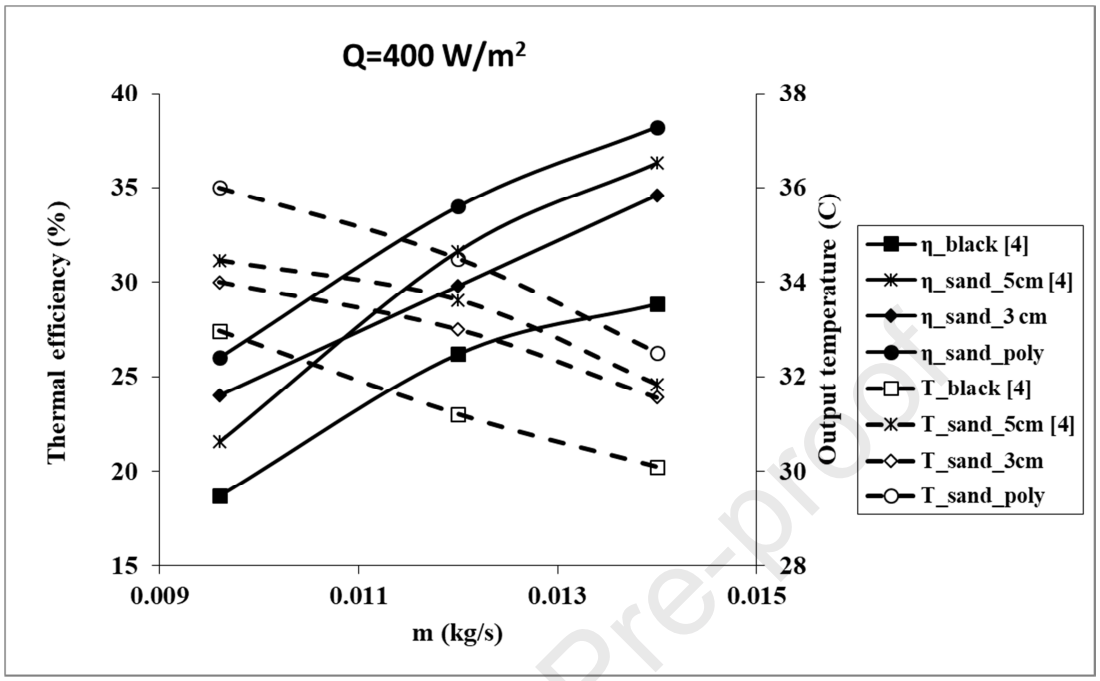

484

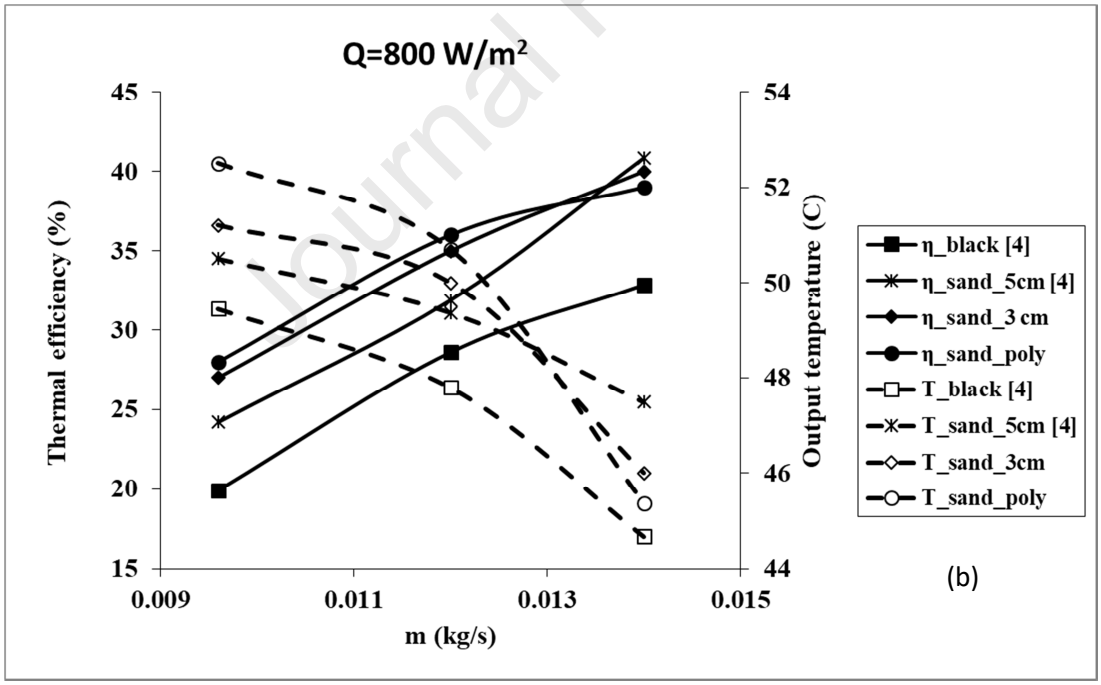

485

486 **Fig. 10. Comparative variation of thermal efficiency and corresponding outlet temperature. (a) *Q*=400**

487 **W/m^2; (b) *Q*=800 W/m^2.**

488

5 Conclusions

The thermal performance characterisation of the sand coated and sand filed (SCSF) polycarbonate sheet based solar air collector (SAC) has been carried out under solar simulated conditions for radiation levels of 400 and 800 W/m^2 and at air flow rates of 0.0096 to 0.0183 kg/s. The results are compared with a solar air collector with a sand coated aluminium absorber under similar test conditions. A charging and discharging time of 180 and 120 min., respectively were determined. The following observations are made:

- The outlet air temperature was found to increase by almost 18 to 25ºC at higher levels of radiation.
- The maximum average storage temperature of SAC was 54ºC and 84 ºC, at solar radiation levels of 400 and 800 W/m^2, respectively.
- Increasing the mass flow rate of the air by 87% resulted in a decrease in the amount of stored energy of SAC by 10 to 24% due to a higher extraction of heat by the flowing air.
- A maximum thermal efficiency of SAC of around 40% and 42% is observed during charging at a mass flow rates of 0.018 kg/s at lower and higher levels of solar radiation, respectively. Furthermore, increase in the mass flow rate by 87% results in enhancement of the thermal efficiency by almost 50 to 53%.
- During discharging, the temperature of the sand comes close to the ambient conditions i.e., at 25 ºC, after 50 to 80 min. at lower level of solar radiation (400 W/m^2), whereas, it takes around 100-120 min. at higher levels of radiation (800 W/m^2).
- Increasing the air mass flow rate from 0.0096 to 0.012 kg/s resulted an increase in the discharging efficiency by almost 15% whereas a reduction up to 9% was observed when the air mass flow rate was 0.0018 kg/s. This is linked with the higher rate of extraction of heat by the flowing air coupled with lower amount of stored heat.
- A reduction in the air gap from 5 cm to 3 cm provided an 11% higher efficiency at lower air mass flow rates for the SAC with the sand coated aluminium based absorber.

The efficiency of the SCSF based on natural sand based SAC was up to 30% higher than that of the SAC with plain aluminium absorber and 20% higher than sand coated aluminium absorber based SAC.

This study establishes the improvement of the thermal performance of the polycarbonate sheet based solar air collector by using thin layer of sand coating on the absorber and with sand filled to act as a storage-cum-collector.

ACKNOWLEDGEMENT:

The authors (specifically Biplab Das) sincerely acknowledges the support received from the DBT, Govt. of India, under NE-Overseas Associateship and also thank Ulster University for hosting and allowing to use the laboratory facilities

References

[1] E. Vengadesan, R. Senthil, A review on recent developments in thermal performance enhancement methods of flat plate solar air collector, *Renew. Sustain. Energy Rev.*, vol. 134 2020.

[2] W. Pang, Y. Cui, Q. Zhang, G.J. Wilson, H. Yan, A comparative analysis on performances of flat plate photovoltaic/thermal collectors in view of operating media, structural designs, and climate conditions, *Renew. Sustain. Energy Rev.*, vol. 119, 2020.

[3] D. R. Tobergte and S. Curtis, "Solar heat worldwide," *J. Chem. Inf. Model.*, vol. 53, no. 9, pp. 1689–1699, 2013.

[4] B. Das, J. D. Mondol, S. Debnath, A. Pugsley, M. Smyth, and A. Zacharopoulos, "Effect of the absorber surface roughness on the performance of a solar air collector: An experimental investigation," *Renew. Energy*, vol. 152, pp. 567–578, 2020.

[5] R. Karwa and V. Srivastava, "Thermal Performance of Solar Air Heater Having Absorber Plate with V-Down Discrete Rib Roughness for Space-Heating Applications," *J. Renew. Energy*, vol. 2013, pp. 1–13, 2013.

[6] S. Debnath, B. Das, P. R. Randive, and K. M. Pandey, "Performance analysis of solar air collector in the climatic condition of North Eastern India," Energy, vol. 165, pp. 281–298, 2018.

[7] A. Karim and M. N. A. Hawlader, "Performance investigation of flat plate, v-corrugated and finned air collectors," Energy, vol. 31, no. 4, pp. 452–470, 2006.

[8] M. Lati, S. Boughali, D. Bechki, H. Bouguettaia, D. Mennouche, N. Gana, S. Ghettas, Experimental investigation on effect of an absorber plate covered by a layer of sand on the efficiency of passive solar air collector, *Int. J. Green Energy*., vol. 16, pp. 413–422, 2019.

[9] S. Singh, S. K. Chaurasiya, B. S. Negi, S. Chander, M. Nemś, and S. Negi, "Utilizing circular jet impingement to enhance thermal performance of solar air heater," *Renew. Energy*, vol. 154, pp. 1327–1345, 2020.

[10] R. Vaziri, M. Ilkan, and F. Egelioglu, "Experimental performance of perforated glazed solar air heaters and unglazed transpired solar air heater," *Sol. Energy*, vol. 119, pp. 251–260, 2015.

[11] P. Velmurugan and R. Kalaivanan, "Energy and exergy analysis of solar air heaters with varied geometries," Arab. J. Sci. Eng., vol. 40, no. 4, pp. 1173–1186, 2015.

[12] E. Ogbonnaya, L. Weiss, Small-scale flat plate collectors for solar thermal scavenging in low conductivity environments, *Int. J. Photoenergy*, 2017.

[13] D. Mercs, A. Didelot, F. Capon, J.F. Pierson, B. Hafner, A. Pazidis, S. Föste, R. Reineke-Koch, Innovative Smart Selective Coating to Avoid Overheating in Highly Efficient Thermal Solar Collectors, *Energy Procedia*., vol. 91, pp. 84-93, 2016.

[14] T. Kiatsiriroat, J. Tiansuwan, T. Suparos, and K. Na Thalang, "Performance analysis of a direct-contact thermal energy storage-solidification," *Renew. Energy*, vol. 20, no. 2, pp. 195–206, 2000.

[15] S. Roy, B. Das, A. Biswas, B.K. Debnath, Energy and Exergy Analysis of a Concrete-Based Thermal Energy Storage System, *J. Inst. Eng. Ser. C.*, vol. 101, pp.517–529, 2020.

[16] G. Kalaiarasi, R. Velraj, M. N. Vanjeswaran, and N. Ganesh Pandian, "Experimental analysis and comparison of flat plate solar air heater with and without integrated sensible heat storage," *Renew. Energy*, vol. 150, pp. 255–265, 2020.

[17] A. Saxena, N. Agarwal, and G. Srivastava, "Design and performance of a solar air heater with long term heat storage," *Int. J. Heat Mass Transf.*, vol. 60, no. 1, pp. 8–16, 2013.

[18] D. V. N. Lakshmi, A. Layek, and P. M. Kumar, "Performance Analysis of Trapezoidal Corrugated Solar Air Heater with Sensible Heat Storage Material," *Energy Procedia*, vol. 109, no. November 2016, pp. 463–470, 2017.

[19] W. Aissa, M. El Sallak, and A. Elhakem, "An experimental investigation of forced convection flat plate solar air heater with storage material," *Therm. Sci.*, vol. 16, no. 4, pp. 1105–1116, 2012.

[20] M. Mohanraj and P. Chandrasekar, "Performance of a forced convection solar drier integrated with gravel as heat storage material," *Proc. IASTED Int. Conf. Sol. Energy, SOE 2009*, no. May 2014, pp. 51–54, 2009.

[21] M. R. I. Ramadan, A. A. El-Sebaii, S. Aboul-Enein, and E. El-Bialy, "Thermal performance of a packed bed double-pass solar air heater," *Energy*, vol. 32, no. 8, pp. 1524–1535, 2007.

[22] G. Murali, K. Rama Krishna Reddy, M. Trinath Sai Kumar, J. SaiManikanta, and V. Nitish Kumar Reddy, "Performance of solar aluminium can air heater using sensible heat storage," *Mater. Today Proc.*, vol. 21, no. xxxx, pp. 169–174, 2020.

[23] M. Abuşka, S. Şevik, and A. Kayapunar, "Experimental performance analysis of sensible heat storage in solar air collector with cherry pits/powder under the natural convection," *Sol. Energy*, vol. 200, 2020.

[24] A. Saxena, G. Srivastava, and V. Tirth, "Design and thermal performance evaluation of a novel solar air heater," *Renew. Energy*, vol. 77, pp. 501–511, 2015.

[25] Y. Dhote and S. Thombre, "Performance Analysis and Parametric Study of a Natural Convection Solar Air Heater With In-built Oil Storage," *J. Inst. Eng. Ser. C*, vol. 97, no. 4, pp. 527–537, 2016.

[26] W. B. Chaouch, A. Khellaf, A. Mediani, M. E. A. Slimani, A. Loumani, and A. Hamid, "Experimental investigation of an active direct and indirect solar dryer with sensible heat storage for camel meat drying in Saharan environment," *Sol. Energy*, vol. 174, pp. 328–341, 2018.

[27] S. B. Prasad, J. S. Saini, and K. M. Singh, "Investigation of heat transfer and friction characteristics of packed bed solar air heater using wire mesh as packing material," *Sol. Energy*, vol. 83, no. 5, pp. 773–783, 2009.

[28] S. Aboul-Enein, A. A. El-Sebaii, M. R. I. Ramadan, and H. G. El-Gohary, "Parametric study of a solar air heater with and without thermal storage for solar drying applications," *Renew. Energy*, vol. 21, no. 3–4, pp. 505–522, 2000.

[29] P. Naphon, "Effect of porous media on the performance of the double-pass flat plate solar air heater," *Int. Commun. Heat Mass Transf.*, vol. 32, no. 1–2, pp. 140–150, 2005.

packed bed solar air heater for a low porosity system," *Sol. Energy*, vol. 74, no. 4, pp. 319–329, 2003.

[31] P. T. Saravanakumar and K. Mayilsamy, "Forced convection flat plate solar air heaters with and without thermal storage," *J. Sci. Ind. Res. (India).* vol. 69, no. 12, pp. 966–968, 2010.

[32] S. Vijayan, T. V. Arjunan, A. Kumar, Exergo-environmental analysis of an indirect forced convection solar dryer for drying bitter gourd slices, Renew. Energy. Vol. 146 pp. 2210–2223, 2020.

Nomenclature:

A_c	Collector area (m^2)
A_{sc}	Area of the absorber (m^2)
$C_{p,s}$	Specific heat of sand (W/m^2K)
$C_{p,a}$	Specific heat of air (W/m^2K)
I	Solar irradiation (W/m^2)
m_a	Air mass flow rate (kg/s)
m_p	Mass of the sensible storage material (i.e., sand) (kg)
Q_{ab}	Absorbed energy by the absorber/storage (W)
Q_{ac}	Accumulated energy (W)
Q_{loss}	Lost energy (W)
Q_u	Useful heat energy gain (W)
$T_{a,out}$	Outlet air temperature (ºC)
$T_{a,in}$	Inlet air temperature (ºC)
$T_{p,average}$	Average temperature of sand air (ºC)
T_e	Temperature of the environment (ºC)
U_c	Overall heat loss coefficient (W/m^2 C)

630 V Air velocity (m/s)

631 $\eta_{s,c}$ Charging efficiency or storing efficiency (-)

632 $\eta_{t,c}$ Thermal efficiency of the collectors (-)

633 $\eta_{t,d}$ Thermal efficiency of the collectors during discharging (-)

634 ρ Density of the air (kg/m^3)

Table 1 Summary of performance of various solar air heaters using sensible heat storage materials.

Reference	Absorber and flow type	Storage material	Cover	Dimensions of the collector	Convection type	Air gap (mm)	Results
Kalaiarasi et al. [16]	Flat aluminium plate black coated; black painted copper fins, single flow	Therminol	Single, glass	2 m × 2 m	Forced	30	η_{therm} was notified 70.8% maximum
Saxena et al. [17]	Flat plate black coated, single flow	Granular carbon	Single, glass	1.51 m × 7 m	Natural and forced	100	η_{therm} was notified 20.7%, 73.6% maximum for natural and forced convection, respectively
Laxmi et al. [18]	Flat plate; trapezoidal groove black coated, single flow	Gravels	Single, glass	2 m × 1 m	Natural	-	η_{therm} was notified 58.16 % maximum for trapezoidal corrugated absorber
Aissa et al. [19]	Flat plate black coated, single flow	Granite stones	Single, glass	2.1 m × 0.84 m	Forced	150	Outlet air temperature was observed 10-25˚C more than ambient air temp.
Mohanraj and Chanderasekar [20]	Copper flat plate black coated, single flow	Sand mixed with aluminium scraps	Single, glass	2 m × 1 m	Forced	25	η_{therm} was estimated about 21%
Ramdan et al. [21]	Flat plate, double flow	Limestone and gravel	Double, glass	-	Forced	120	η_{therm} with gravel or limestone as SHM was improved by 28.3% and 25.6% , respectively than system without SHM
Murali et al. [22]	Aluminium can, single flow	Aluminium scrapes and pebble stones	Single, glass	1.36 m × 0.76 m × 0.0125 m	Forced	-	η_{therm} was notified 69.8% maximum for aluminium scrapes as SHM
Abuska et al. [23]	Flat plate black coated, single flow	Cherry pits/powder	Single, glass	1 m × 2 m × 0.2 m	Natural	120	η_{therm} was notified 27.1 % maximum
Saxena et al. [24]	Flat plate black coated	Dessert sand and granular carbon	Single, glass	1.51 m × 0.70 m	Natural and forced	100	η_{therm} was notified 20.7 % and 80.1% maximum for natural and forced convection, respectively
Dhote and Thombre [25]	Flat copper plate	Unused engine oil	Single, glass	2 m × 1m	Natural	40	Highest overall efficiency of 16.8% was reported

Chaouch et al. [26]	Flat plate black coated	Pebbles	Glass	-	Forced	-	η_{therm} of solar collector was improved 28 % than system without SHM
Prasad et al. [27]	Flat plate with two different ducts	Wire mesh	Double, glass	1.65 m × 0.4 m	-	25	53.3% to 68.5% improvement was noticed in η_{therm}
Aboul-Enein et al. [28]	Flat plate black coated	Sand, granite and water	Single, glass	-	Natural	-	Outlet air temperature was observed highest for sand
Naphon [29]	Flat plate, double flow	Porous media	Single, glass	-	-	-	η_{therm} was improved 25.9% than SAH without porous media
Thakur et al. [30]	Flat plate black coated with two different ducts	Wire screen matrix	Double, glass	2.4 m × 0.4 m	Forced	25	Improved heat transfer rate was noticed
Saravanakumar and Mayilsamy [31]	Flat plate black coated, double flow	Sand, sand with iron scraps, gravel and gravel with iron scraps	Single, glass	0.3 m × 0.3 m	Forced	25	η_{therm} and outlet air temperature was improved by10-20% than SAH without storage media
Vijayan et al. [32]	corrugated plate black coated	Pebbles	Single, glass	2 m × 1 m	Forced	30	Maximum exergy efficiency of 54.3% was achieved

* η_{therm} –thermal efficiency (%)

Highlights

- Sand filled sand coated (SCSF) polycarbonate based solar collector is presented
- Efficiency of sand storage based collector and aluminium collector is compared
- 87% increase in mass flow rate of air lead to 10-24% decrease in stored energy
- Reduction of air gap to 3 cm leads to 11% higher efficiency of aluminium plate based collector
- SCSF polycarbonate sheet based absorber provides 39% higher thermal efficiency

Declaration of interests

☐ The authors declare that they have no known competing financial interests or personal relationships that could have appeared to influence the work reported in this paper.

☐The authors declare the following financial interests/personal relationships which may be considered as potential competing interests:

There is no conflicts of interest

Dr. Biplab Das
Post. Doc.
Belfast School of Architecture and the Built Environment
Centre for Sustainable Technologies, 26B03
Ulster University, Northern Ireland, UK
BT37 0QB

Experimental Performance Analysis of a Novel Sand Coated and Sand Filled Polycarbonate Sheet Based Solar Air Collector

Credit author statement

Biplab Das: Done the experiment and make the draft manuscript

Jayanta Deb Mondol: Revision of the draft manuscript and analysis of the results

Sushant Negi: Preparation of the draft manuscript

Mervyn Smyth: Analysis of the results and revision of the manuscript

Adrian Pugsley: Analysis of the results and revision of the manuscript